PDF Calculations of Piloted Turbulent Nonpremixed Flames of Methane

A. R. MASRI

Department of Mechanical Engineering, University of Sydney, Sydney, Australia

and

S. B. POPE

Sibley School of Mechanical and Aerospace Engineering, Cornell University, Ithaca, NY

A *velocity-composition joint pdf* transport equation has been solved by the Monte Carlo method to calculate the structure of pilot-stabilized turbulent nonpremixed flames of methane. Three components of velocity and a conserved scalar, namely, mixture fraction, ξ are jointly represented in the pdf. A new model is used for turbulent frequency. Turbulent dissipation and the fluctuating pressure gradient terms are conditionally modeled. Two simple models for thermochemistry are used. In one, density is a piecewise function of ξ, and in the other, density is obtained from calculations of a laminar counterflow diffusion flame of methane with a stretch rate, $a = 100\ s^{-1}$. Calculations are compared with the corresponding experimental measurements performed on a number of flames ranging from flames with low mixing rates to ones close to extinction.

The velocity, turbulence, and mixing fields are predicted with reasonable accuracy down to $x/D_j \sim 30$. The agreement with experiments is less satisfactory at $x/D_j = 50$. This will improve with the use of better pdf models which have recently been developed [27, 30, 31]. The reactive scalars are very well predicted only for flames which are far from extinction. This is expected considering the simplicity of the thermochemical model. This paper is a first step towards implementing realistic chemistry in the code, and hence predicting the observed finite rate kinetic effects in these flames.

INTRODUCTION

In recent years, the conserved scalar approach [1] has been well established as a method for calculating a class of turbulent reacting flows with fast chemistry. The usefulness of this approach lies in the fact that the reactive scalars are (by assumption) single-valued functions of a conserved scalar, namely, the mixture fraction, ξ. Faeth and Samuelsen [2] review the various models which adopt this approach and refer to various measurements in turbulent flames close to equilibrium. In most practical combustors, however, the chemical kinetics are not so fast, and consequently, the reactive scalars are no longer uniquely determined by the mixture fraction. Janicka and Kollmann [3] used two variables to account for finite rate kinetic effects in turbulent flames of hydrogen, and Bilger and Stårner [4] adopted a three variable formulation for hydrocarbon fuels. With such approaches, the closure problem for the mean reaction rate has to be addressed. Janicka and Kollmann [3] modeled the joint probability density functions (pdf) of the two variables in terms of their first and second

Published by Elsevier Science Publishing Co., Inc.
655 Avenue of the Americas, New York, NY 10010

0010-2180/90/$3.50

moments, while Bilger and Stårner [4] developed an expression for the mean reaction rate in terms of the first moments only.

Such approaches have been relatively successful in flows where the deviations from fast chemistry are not too large. They fail, however, to predict the correct flame structure at significant departures from equilibrium, and certainly fail to predict flame extinction, these being necessary requirements for a generally-applicable combustion model. It is evident that, to satisfy these needs, realistic chemistry should be considered in the models. Detailed chemical kinetic schemes are, of course, too complicated to be included directly in turbulent flame calculations. The short mechanisms which can be systematically reduced from the detailed ones are extremely useful in this context. Bilger et al. [5] and Peters [6] have reduced the detailed chemical kinetic scheme for methane to four-step mechanisms which predict correctly laminar flame structure as well as extinction. The use of such schemes in turbulent flame calculations means that five variables need to be considered to describe the scalar fields.

In problems where such a large dimensionality is necessary, the probability density function approach is extremely useful. Consider a set of $\sigma \geq 1$ composition variables $\Phi = \phi_1, \phi_2, \ldots, \phi_\sigma$, and let the σ-dimensional sample-space corresponding to these variables be $\Psi = \psi_1, \psi_2, \ldots, \psi_\sigma$. Define, at a particular location in space $\boldsymbol{x}$ and time t, the composition joint pdf of Φ, $f_\phi(\Psi; \boldsymbol{x}, t)$ as the probability density function of the joint event $\Phi(\boldsymbol{x}, t) = \Psi(\boldsymbol{x}, t)$. The mean of any function $\langle Q(\Phi) \rangle$ can be determined from the joint pdf, $f_\Phi(\Psi; \boldsymbol{x}, t)$ by

$$\langle Q(\Phi) \rangle = \int f_\Phi(\Psi; \boldsymbol{x}, t) Q(\Psi) d\Psi, \qquad (1)$$

where integration is over the whole composition space. The major advantage of this approach is that the *composition joint pdf* contains all the statistical information required to determine the mean reaction rate. Another advantage is that the chemical reaction term in the pdf transport equation appears in closed form and does not require modeling. Turbulent mixing and transport still need to be modeled.

Considering the large dimensionality of the joint pdf's, it is clear that analytic solutions are generally impossible and numerical methods are required. Janicka *et al.* [7] have obtained finite-difference solutions for $f_\phi(\psi_1; x_1, x_2)$, but these methods also become impractical when the dimensionality of the problem increases, such as is the case with turbulent reacting flows close to extinction. The Monte Carlo method, on the other hand, is well-suited for such problems. Pope [8] proposes a solution algorithm for the composition joint pdf which has been used for calculating premixed propane–air flames [9] and diffusion flames of H_2 [10]. Chen et al. [11, 12] used this method to calculate finite-rate kinetic effects in nonpremixed flames of methane and propane.

A major disadvantage of the composition joint pdf approach is that the velocity and turbulence fields are determined separately and turbulent transport terms have to be modeled. This is overcome by using the velocity-composition joint pdf, $f(V, \Psi; \boldsymbol{x}, t)$ where $V = V_1, V_2, V_3$ are the three independent velocity variables corresponding to three components of velocity $\boldsymbol{U}$. At a given location in space and time, f is the probability density of the compound event $\boldsymbol{U}(\boldsymbol{x}, t) = V$, and $\Phi(\boldsymbol{x}, t) = \Psi(\boldsymbol{x}, t)$. In the transport equation for $f(V, \Psi; \boldsymbol{x}, t)$, all one-point processes such as convection, buoyancy, and chemical reaction appear in closed form regardless of the complexity and the nonlinearity of the reaction scheme [13]. Viscous dissipation, fluctuating pressure gradient, and molecular diffusion need to be modeled. Pope [13] gives a detailed description of the models used and describes a Monte Carlo method to solve the velocity-composition joint pdf equation for the general case. With this approach, it becomes possible, in principle, to predict flame extinction as well as the correct structure of turbulent reacting flows with large or small departures from chemical equilibrium. Pope and Correa [14] have used two composition variables (mixture fraction, ξ and a reaction progress variable, η) and solved for the joint velocity-ξ-η pdf in axisymmetric syngas nonpremixed flames far from equilibrium. For the same flames, Haworth *et al.* [15, 16] have adopted flamelet modeling using a library of laminar flamelet solutions with a range of stretch rates. They solved the velocity-mixture

fraction pdf and calculated the scalar dissipation, and hence the stretch rate from the first and second moments of ξ assuming a lognormal distribution for the scalar dissipation pdf.

Experimental studies of turbulent nonpremixed flames of methane close to extinction have been reported by Masri *et al.* [17–19]. The burner which produces the flame consists of a central jet of fuel surrounded by a larger annulus of coflowing premixed combustion products, and this is centered in a much larger coflowing stream of air. This arrangement has been designed to allow the study of strong turbulence effects on the chemistry under conditions approaching extinction in a flow which is fluid-dynamically simple: a streaming flow describable by parabolic equations. Extinction is approached by increasing the fuel jet velocity: when extinction occurs, it leaves the pilot annulus alight with apparently some mixing and combustion of the fuel and outside air occurring over the first 15 diameters, but not at a sufficient rate of heat release to propagate the flame further. At jet velocities below the extinction condition, the flame develops into a full turbulent jet diffusion flame with a region near x/D_j of 20 where mixing is intense (D_j is the fuel jet diameter), temperatures are lowest, and combustion conditions are most critical.

Measurements show that for methane flames approaching extinction, lean fluid mixtures are either burnt or unburnt, and consequently, the pdf's of the reactive scalars are bimodal. Local extinction becomes increasingly significant as the flame approaches blowoff. The flame is kept alight by fully burnt pockets or streaks of fluid and global blowoff occurs when the frequency of occurrence of these pockets decreases below a critical value. For rich fluid mixtures, the pdf's of the reactive scalars are monomodal and widely distributed between the limits of fully reacted and fully nonreacted, i.e., frozen. The centroid of these rich distributions gradually shifts towards the frozen limits as the flame approaches extinction. These findings raise questions regarding the spatial structure of the flames near extinction. Are the reaction zones thin and laminar or broad and distributed with turbulence within them? The laminar flamelet models [15, 16, 20, 21] assume that the reaction zone is thinner than the smallest scale of turbulence and conceive the turbulent flame as an ensemble of thin moving laminar flamelets.

The piloted flame geometry is very useful for the study of turbulence–chemistry interactions including local extinction. The experiments performed have generated much information and, as indicated above, they have raised several questions. Our goal (beyond this paper) is to apply the velocity-composition joint pdf approach to these flames using a four-step mechanism to describe the chemistry. A comparison of measured and calculated statistics is likely to lead to increased understanding of the important processes and to improved pdf models.

In this paper, the first step is taken towards the goal stated above. The velocity-composition joint pdf approach is applied to the piloted diffusion flame, but with a very simple, conserved-scalar thermochemical model. Because of the over-simple thermochemical model, questions of flame structure and extinction cannot be addressed. Rather, the objectives of this paper are: to describe the application of the pdf method to this flame; to compare calculated and measured mean velocity and turbulence statistics (which depend only weakly on the thermochemical model); and to compare the calculated and measured profiles of mean density, temperature, etc., to illustrate the deficiencies of the conserved-scalar thermochemical model for flames close to extinction.

Density is determined by two methods: (i) as a piecewise function of mixture fraction, and (ii) from a look up table for the calculated properties of a laminar counterflow [22] nonpremixed flame of methane with a stretch rate of $a = 100\ \text{s}^{-1}$. It should be noted that the use of laminar flamelet properties do not in this case imply that reaction zones are thin. It is intended only to demonstrate the adequacy (or lack of it) of the approach at various flow conditions. A new method for calculating the turbulent frequency to suit the new flow geometry is also described.

EXPERIMENTAL DATA

The piloted burner developed at the University of Sydney has a central jet of fuel, 7.2 mm in diameter surrounded by a stoichiometric premixed

and fully burnt annulus of C_2H_2, H_2, and air with the C/H ratio adjusted to be the same as that of the fuel. The outer diameter of the annulus is 18.0 mm and the lips are thin. The annulus of combustion products from the pilot shields the fuel issuing from the central jet and extends for about 4 fuel jet diameters, allowing for any unburnt reactants in the pilot stream to be consumed. During all the measurements, the coflow air stream velocity, $\bar{u}_e$ and the pilot burnt gas velocity, $\bar{u}_{pb}$ are maintained at 15 and 24 m/s, respectively. The pilot burnt gas velocity $\bar{u}_{pb}$ is calculated from known reactant flow rates assuming a product temperature of 2600 K. The flame characteristics are then changed by varying the methane bulk jet velocities $\bar{u}_j$.

Masri and Bilger [23] report thermocouple measurements of temperatures, LDA measurements of velocity and turbulence and composition measurements by sample probe. The measurements were made with CNG (compressed natural gas, 90.9% CH_4 by volume) and LPG (liquefied petroleum gas 88.0% C_3H_8 by volume) fuels at the University of Sydney. A slightly different version[1] of the burner has been installed at the Turbulent Diffusion Flame Facility, at Sandia National Laboratories, Livermore. Space- and time-resolved measurements of temperature, density, mixture fraction, and the mass fractions of CH_4, O_2, H_2O, H_2, CO, CO_2, and N_2 have been obtained by pulsed spontaneous Raman and Rayleigh scattering in the blue (visibly soot-free) regions of pure methane flames. These data have been reported in Masri *et al.* [17–19]. Table 1 shows the various flames investigated experimentally and indicates the type of measurements available for each flame. In this paper, calculations are made for methane flames at the conditions listed in Table 1 and the results are compared with the relevant experimental data. Here, x is the distance from the burner's exit plane and D_j is the central jet diameter. Extinction of the flame occurs in the intensely-mixed shear layer extending from $x/D_j \simeq 15$ to 35, at $\bar{u}_j = 65$ m/s.

[1] The outside of the Sandia burner is not smoothly profiled like the one at Sydney University. Although this causes some differences in the air-side boundary layer, the overall flame characteristics remain identical.

TABLE 1

Investigated Pilot-Stabilized Diffusion Flames of CH_4

Flame	$\bar{u}_j$ (m/s)	LDA	Probe	Raman	Characteristics
K	27	√	√		All yellow, electrically connected.[a]
L	41	√	√	√	Blue to $x/D_j \simeq 30$, electrically connected.
M	55	√	√	√	Almost all blue, electrically intermittent.

[a] The flame is electrically connected when a continuous signal is recorded for the current conducted between a simple wire grid placed at $x/D_j = 70$ in the flame and the nozzle with a 20 V imposed potential difference. It is electrically intermittent when intermittency spikes start to appear in the recorded current signal.

Conventional averages are presented for the velocity and the temperatures measured by the Raman technique, and Favre averages are shown for the species mass fractions. Thermocouple measurements of temperature are close to conventional averages. It is still not definite, however, whether probe sampling data are closer to the conventional or Favre averages. Masri *et al.* [17] compare probe measurements of species mass fractions with the corresponding conventional and Favre averages of the data collected by the Raman technique. The comparisons are not conclusive.

MODELING

Joint PDF Equation

The joint pdf, $f(\boldsymbol{V}, \Psi; \boldsymbol{x}, t)$ is the probability density of the joint events $\boldsymbol{U}(\boldsymbol{x}, t) = \boldsymbol{V}$ and $\Phi(\boldsymbol{x}, t) = \Psi$. It contains a complete one-point statistical description of velocity and composition in a turbulent reacting flow [13]. If $Q(\boldsymbol{U}, \Phi)$ is any function of $\boldsymbol{U}$ and Φ, then its mean value at any given location in space and time, $(\boldsymbol{x}, t)$ can be determined from the joint pdf by

$$\langle Q(\boldsymbol{x}, t)\rangle = \int\int Q(\boldsymbol{V}, \Psi) f(\boldsymbol{V}, \Psi; \boldsymbol{x}, t)\, d\boldsymbol{V}\, d\Psi, \tag{2}$$

where $\int d\boldsymbol{V}$ represents integration over the three-dimensional velocity space and $\int d\Psi$ represents

integration over the σ-dimensional composition space.

In turbulent reacting flows, the transport equation for the *velocity-composition joint pdf*, $f(V, \Psi; x, t)$ is

$$\rho(\Psi)\frac{\partial f}{\partial t} + \rho(\Psi)V_j\frac{\partial f}{\partial x_j} + \left(\rho(\Psi)g_j - \frac{\partial \langle p\rangle}{\partial x_j}\right)\frac{\partial f}{\partial V_j} + \frac{\partial}{\partial \psi_\alpha}[\rho(\Psi)S_\alpha(\Psi)f] = \frac{\partial}{\partial V_j}\left[\left\langle -\frac{\partial \tau_{ij}}{\partial x_i} + \frac{\partial p'}{\partial x_j}|V, \Psi\right\rangle f\right] + \frac{\partial}{\partial \psi_\alpha}\left[\left\langle -\frac{\partial J_i{}^\alpha}{\partial x_i}|V, \Psi\right\rangle f\right]. \quad (3)$$

In this equation, g_j is the body force (per unit mass) in the x_j direction; $\langle p\rangle$ and p' are the mean and fluctuating pressure; S_α is the source term for species α due to chemical reaction; τ_{ij} is the sum of the viscous and viscous-diffusive stress tensors, and $J_i{}^\alpha$ is the diffusive mass flux of species α in the x_i direction. The density $\rho(\Psi)$ and the reaction source terms, $S(\Psi)$, are known functions. All the terms on the left-hand side appear in closed form, while those on the right-hand side need to be modeled. ($\langle Q|V, \Psi\rangle$ denotes the mean of Q conditional upon the events $U(x, t) = V$ and $\Phi(x, t) = \Psi$.)

In the flames studied in this paper, only one scalar variable (mixture fraction, ξ) is considered along with three components of velocity, U. One-point statistics of these dependent variables are functions of the axial and the radial coordinates, x and r only. Dependence of statistics on time, t and on the circumferential coordinate, θ, is eliminated because the flow is statistically axisymmetric and stationary. All thermochemical quantities are assumed to be single functions of ξ and can be determined from the joint pdf of velocity and ξ. The mean density is

$$\langle \rho(x, r)\rangle = \int\int \rho(\xi) f(V, \hat{\xi}; x, r)\, dV\, d\hat{\xi} \quad (4)$$

where V and $\hat{\xi}$ are the independent velocity and composition variables. The density-weighted joint pdf, $\tilde{f}(V, \hat{\xi})$ is given by

$$\tilde{f}(V, \hat{\xi}) = \rho(\hat{\xi}) f(V, \hat{\xi})/\langle \rho\rangle. \quad (5)$$

The transport equation for the density-weighted joint pdf is solved and the Favre (or density-weighted) means are then determined as follows:

$$\tilde{Q} = \langle \rho Q\rangle/\langle \rho\rangle = \int\int \tilde{f}(V, \hat{\xi}) Q(V, \hat{\xi})\, dV\, d\hat{\xi}. \quad (6)$$

Calculated and Favre means are used for comparison with the experimental data presented in this paper.

PDF Models

The conditional modeling described by Pope [24] is adopted here with the mixture fraction, ξ, used to differentiate between turbulent and nonturbulent fluid. Three processes describe the interactions between the turbulent and irrotational fluid: entrainement, momentum exchange, and energy exchange. A constant is assigned to the modeling of each of these processes, $C_g = 1.5$, $C_m = 1.5$, and $C_e = 5.0$. Within the turbulent fluid, dissipation and the effects of fluctuating pressure are modeled, respectively, by the improved stochastic mixing model [25] with a constant $C_u = 1.0$, and the stochastic reorientation model [26] with a constant $C_R = 4.5$. Scalar dissipation is accounted for by the improved stochastic mixing model [24] which is similar to that used for turbulent kinetic energy with a constant $C_\phi = 2.0$ being the ratio of the velocity to scalar time scales. The model allows for correlated mixing in velocity and composition space and the constant $C_{u\phi} = 1.0$ is used to define the degree of correlation [13].

Turbulent Frequency

The turbulent frequency ($\omega = \epsilon/k$) determines the rate at which the processes described above occur. It is assumed here, as in previous calculations of free shear flows [24, 27], that the turbulent time scale is constant across the flow. In self-similar free shear flows [27], the turbulent frequency is given by $\omega = C'_\omega \Delta\langle u\rangle/\delta$ where $\Delta\langle u\rangle$ is the characteristic mean velocity difference and

δ is the characteristic flow width. This is not applicable for the piloted flame geometry considered here because it does not account for the shear layers on the fuel and air sides of the pilot stream. A more appropriate formulation is

$$\omega = C_\omega \int_0^\infty \left(\frac{\partial \langle u \rangle}{\partial r}\right)^2 dr \Big/ \int_0^\infty \left(\left|\frac{\partial \langle u \rangle}{\partial r}\right|\right) dr \tag{7}$$

where C_ω is a constant. With this expression, the decay of ω with axial distance is almost exponential which is realistic for turbulent jets.

The value of C_ω is selected to give the best agreement between experiments and calculations. A value of $C_\omega = 0.3$ is used for all subsequent calculations as it gives the closest agreement with the measured velocity, turbulence, and mixing fields for all flames K, L, and M. The results are presented in a later section of this paper.

Thermochemical Models

In the low Mach number flows considered in these calculations, the thermochemistry influences the velocity and mixing fields through density effects only. Two methods are used to determine the density of each fluid particle.

Method I: Density is a piecewise function of mixture fraction;

$$\frac{1}{\rho(\xi)} = \frac{\xi_s}{\rho|_{\xi=0}\xi_s + (\rho|_{\xi_s} - \rho|_{\xi=0})\xi} \quad \text{for } \xi < \xi_s$$

$$\frac{1}{\rho(\xi)} = \frac{1-\xi_s}{\rho|_{\xi_s} - \rho|_{\xi=1}\xi_s + (\rho|_{\xi=1} - \rho|_{\xi_s})\xi} \quad \text{for } \xi > \xi_s \tag{8}$$

where ξ_s is the stoichiometric value of mixture fraction and $\xi_s = 0.055$ for methane.

Method II: A look up table is generated for density as a function of mixture fraction from the laminar flame calculations of Miller *et al.* [22] for a counterflow diffusion flame with a stretch rate, $a = 100\ s^{-1}$. Extinction for such flames occurs at $a = 360\ s^{-1}$. As stretch rates increase from $a = 1\ s^{-1}$ to $360\ s^{-1}$, temperature and species mass fractions change only moderately. The selected value of $a = 100\ s^{-1}$ is intermediate. Temperature and the mass fraction of stable species are also tabulated as a function of ξ. By interpolating in these tables, the thermodynamic properties are assigned to each particle at its value of ξ. Figure 1 shows profiles of density versus mixture fraction for three laminar flamelets of CH_4 with stretch rates of $a = 5\ s^{-1}$, $100\ s^{-1}$, and $350\ s^{-1}$. Density obtained from Equation 8 is also shown. It is noted that the variation in density with increasing stretch rate is insignificant. The difference between the density of laminar flamelets and that obtained from Eq. 8 is small around stoichiometric, but increases on either side of ξ_s.

SOLUTION PROCEDURE

The Monte Carlo method is used to solve the transport equation for the density-weighted velocity-composition joint pdf which is represented by a large number (N) of notional particles. Since the flow is parabolic, the solution is obtained by marching in the axial direction, x. At any axial location, each particle has a radial position, velocity, and mixture fraction, ξ. The value of ξ is used to determine the density of each fluid par-

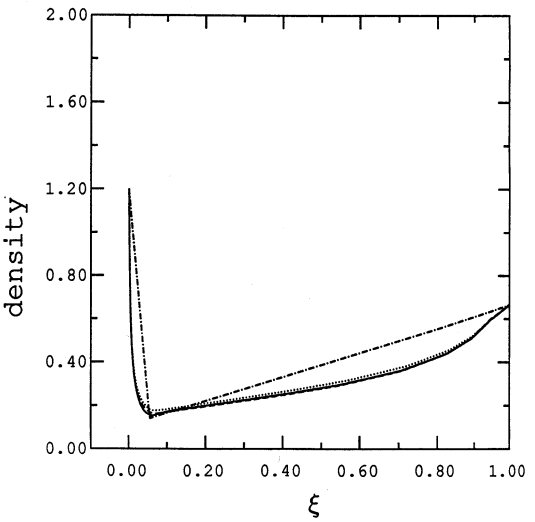

Fig. 1. Density versus mixture fraction obtained from the laminar flamelet calculations [22] of counterflow diffusion flames of methane at various stretch rates, a: —— $a = 5\ s^{-1}$; ---- $a = 100\ s^{-1}$; ····· $a = 350\ s^{-1}$. The line -·-·- is for density as a piecewise function of ξ given by Eq. 8.

ticle by one of the two thermochemical models described above.

Because the number of particles used in the calculations is finite, the Monte Carlo method results in a random sampling error [8] which has an expected value of zero indicating that the method is not biased with N. However, using the composition pdf approach to calculate turbulent nonpremixed flames of hydrogen, Nguyen and Pope [10] found that a small bias exists for small N. Haworth and Pope [28] obtained a definite bias with N using the velocity-composition pdf approach for plane mixing layers. Pope [8] demonstrated that the calculated averages converge to the true averages as the number of particles tends to infinity. This is true regardless of the dimensionality of the pdf. For a scalar ϕ, the statistical error decreases with the square root of N and is likely to be proportional to the standard deviation, $\langle \phi'^2 \rangle^{1/2}$. In their analysis of turbulent diffusion flames, Nguyen and Pope [10] estimated the standard error on mixture fraction as

$$\epsilon \sim 3.0 \left(\frac{\langle \xi'^2 \rangle}{N} \right)^{1/2}. \tag{9}$$

To illustrate the decrease in the statistical error with increasing N, calculations were repeated for flame L with different values of N: 8000, 24 000, and 48 000. Figure 2 shows four plots with three radial profiles on each plot for the different values of N. Radial profiles for the mean axial velocity $\langle u \rangle$ and its rms of fluctuations, $\langle u'^2 \rangle^{1/2}$ are shown for $x/D_j = 20$ and those for $\langle \xi \rangle$ and $\langle \xi'^2 \rangle^{1/2}$ are shown for $x/D_j = 50$ in flame L. Note that for convenience, $\langle u'^2 \rangle^{1/2}$ and $\langle \xi'^2 \rangle^{1/2}$ will be referred to as $\langle u' \rangle$ and $\langle \xi' \rangle$, respectively. The profiles for $N = 8000$ deviate slightly from those of $N = 24\,000$ and 48 000 which almost overlap. Doubling the number of particles from 24 000 to 48 000 leads to a slight decrease in sampling error and to a very little gain in accuracy, while the CPU time, which increases linearly with N, almost doubles. By doubling the number of particles from 25 000 to 50 000, Haworth and Pope [28] decreased the sampling error in the plane mixing layer calculation of $\langle uv \rangle$ by about 2%.

The results presented in the remainder of this paper are obtained with $N = 24\,000$ particles. At each axial location, mean quantities, both conditional and nonconditional, are obtained by the method of cross-validated least squares cubic splines [29]. This method is superior to simple ensemble averaging as it reduces the statistical error [25]. All computations are performed on a VAX 11/780 and are restricted to $x/D_j \leq 50$ for all flames. With about 200, 300, and 400 steps for flames K, L, and M, the CPU times required are approximately 370, 560, and 740 minutes, respectively.

Initial and Boundary Conditions

The initial conditions (at the jet exit plane) and boundary conditions (in the coflowing stream) are specified for the mean mixture fraction, $\langle \xi \rangle$, the mean velocities $\langle u \rangle$, $\langle v \rangle$, and $\langle w \rangle$, and the variances and covariances for the velocities. The variance of ξ is zero. From these first and second moments, the velocity-composition joint pdf is specified to be joint normal at the boundaries. Figure 3 shows the measured and specified initial conditions for $\langle u \rangle$ and $\langle u' \rangle$. Profiles for $\langle u \rangle$ are approximated by power law fits (in the jet and coflow), while those for $\langle u' \rangle$ are piecewise linear. Sharp changes in $\langle u \rangle$ are intentionally avoided for computational purposes. Although the specified velocities may deviate slightly from the measured ones, the momentum both in the jet and the coflow streams are within $\pm 2\%$ of the momentum at the specified conditions. The net momentum deficit in the coflow stream due to the boundary layer is $\sim$110 kgm/s^2 which is about 32% of the total measured momentum of the coflow air in an annulus bounded by $r/R = 7$. Initial radial and circumferential velocities are taken as zero, $\langle v \rangle = \langle w \rangle = 0$. It is also assumed that the initial profiles of $\langle v' \rangle$ and $\langle w' \rangle$ are identical to those of $\langle u' \rangle$. The covariances are taken as $\langle u'v' \rangle = \langle v'u' \rangle = C_{cv}(\langle u'^2 \rangle \langle u'^2 \rangle)^{1/2}$, where C_{cv} is a constant equal to 0.5. All other covariances are zero.

The mean mixture fraction is taken to be one in the jet stream and stoichiometric, $\langle \xi \rangle = \xi_s = 0.055$ in the pilot stream. In the coflowing air stream, ξ is set equal to a very small positive value

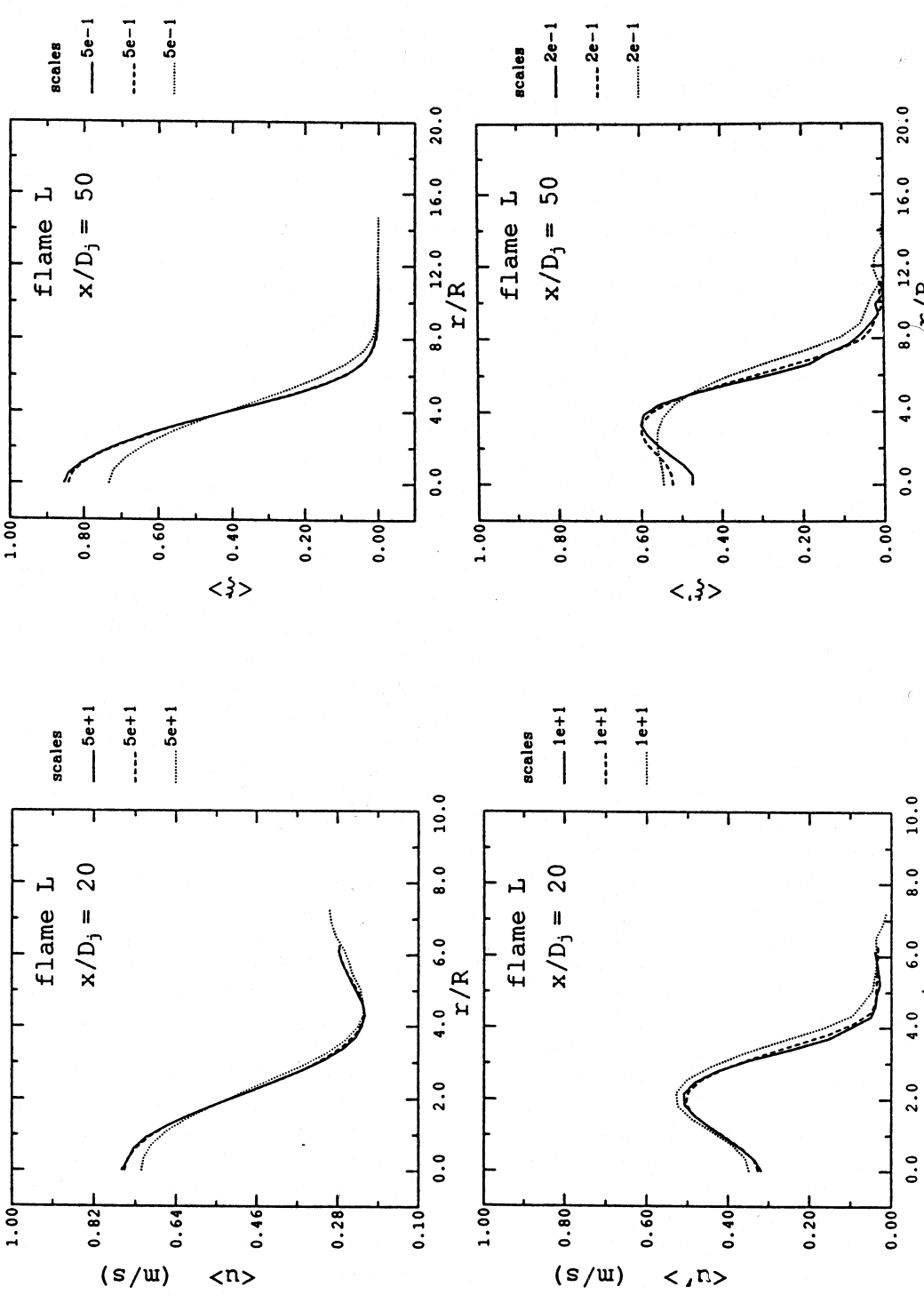

Fig. 2. Radial profiles at various axial locations in the flames for $\langle u \rangle$, $\langle u' \rangle$, $\langle \xi \rangle$, and $\langle \xi' \rangle$ calculated with a various number of notional particles, N: —— $N = 48\,000$; - - - - $N = 24\,000$; ..... $N = 8000$.

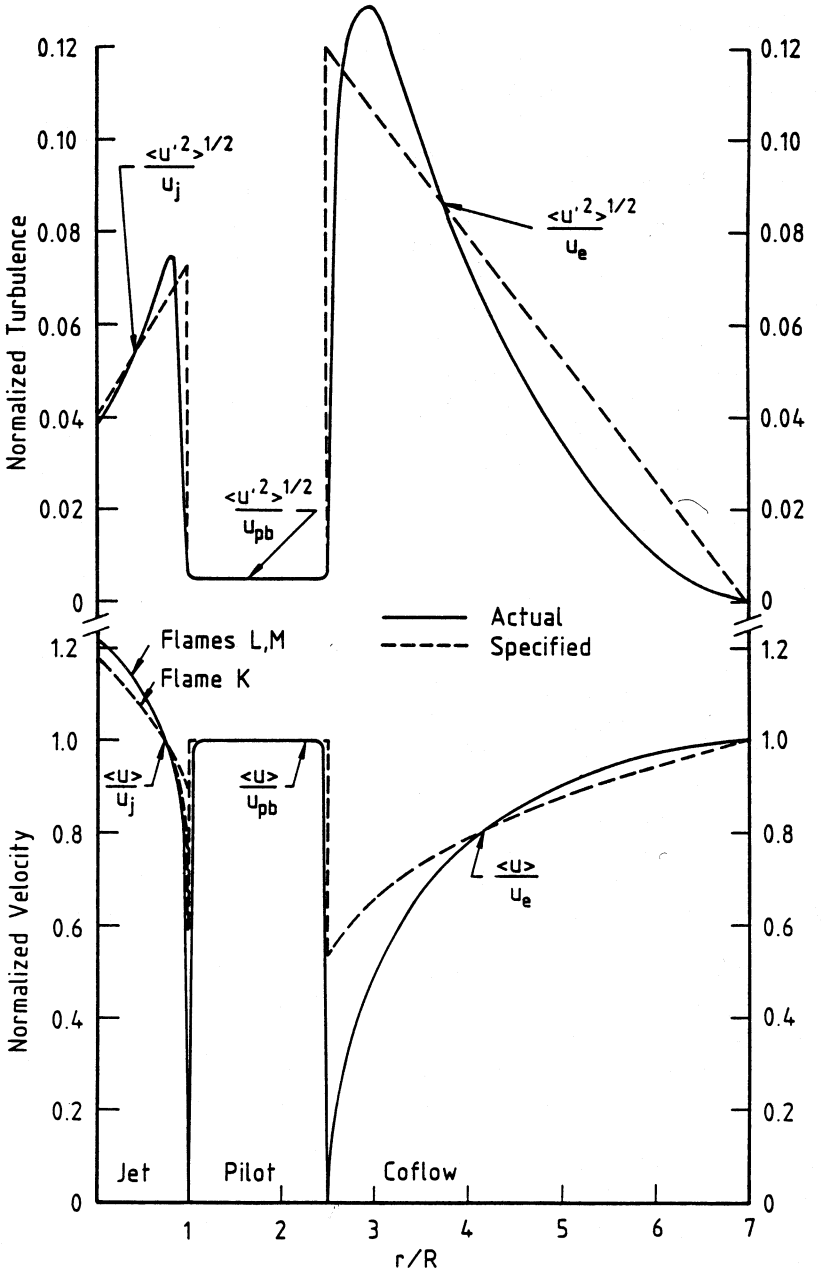

Fig. 3. Actual and specified initial conditions for the mean axial velocity $\langle u \rangle$ and its rms of fluctuations, $\langle u'^2 \rangle^{1/2}$.

for particles within the coflow turbulent boundary layer which extends to $r/R = 7$ where $R = 3.6$ mm is the fuel jet radius. The mixture fraction is zero for particles located at $r/R > 7$. This boundary condition is used to differentiate between turbulent ($\xi > 0$) and nonturbulent ($\xi = 0$) fluid. The covariances of ξ are set to zero. The Monte Carlo solution was found to be fairly insensitive to the slight differences between the specified and actual initial profiles.

The particles used in the calculation are initially distributed along a solution grid which covers the pilot stream, and part of the jet and air streams. The grid expands with axial distance towards both the jet centerline and the air stream. The inner and outer edges of the grid are determined at each axial location by comparing the mean density profile to the density specified at the boundaries. The jet centerline is the limit of expansion for the inner boundary of the grid. At the inner boundary of the jet, conditions are specified as for the initial conditions at the corresponding radial location of the boundary. Conditions at the outer boundary are specified similarly if the outer edge of the jet is located within $r/R < 7$. When the outer boundary exceeds $r/R = 7$, $\langle u \rangle$ is set to the coflow value and all other velocities, variances, and covariances are set to zero.

RESULTS AND DISCUSSION

Comparisons with the experimental results for density, velocity, turbulence, and mixing fields for flames K, L, and M are made with the calculations from method I where density is considered to be a piecewise function of mixture fraction ξ. These calculations are almost identical to those of method II for the same flames. In method II, the properties at each value of ξ are looked up from a table of properties for a methane laminar counterflow diffusion flame with a stretch rate of 100 s^{-1}. The measured reactive scalars like temperature and species mass fractions are compared with the calculations from method II. For the reactive and conserved scalars, the experimental results presented for flame K are from probe measurements, while those for flame M are from Raman measurements. A mix of probe and Raman measurements is presented for flame L.

Statistics of Velocity, Mixture Fraction and Density

Except for Fig. 7, each of Figs. 4–1 shows three plots for flames K, L, and M, respectively, comparing experimental results with calculations. All the figures are plotted with respect to normalized radial distance, r/R. Figs. 4 and 5 show radial

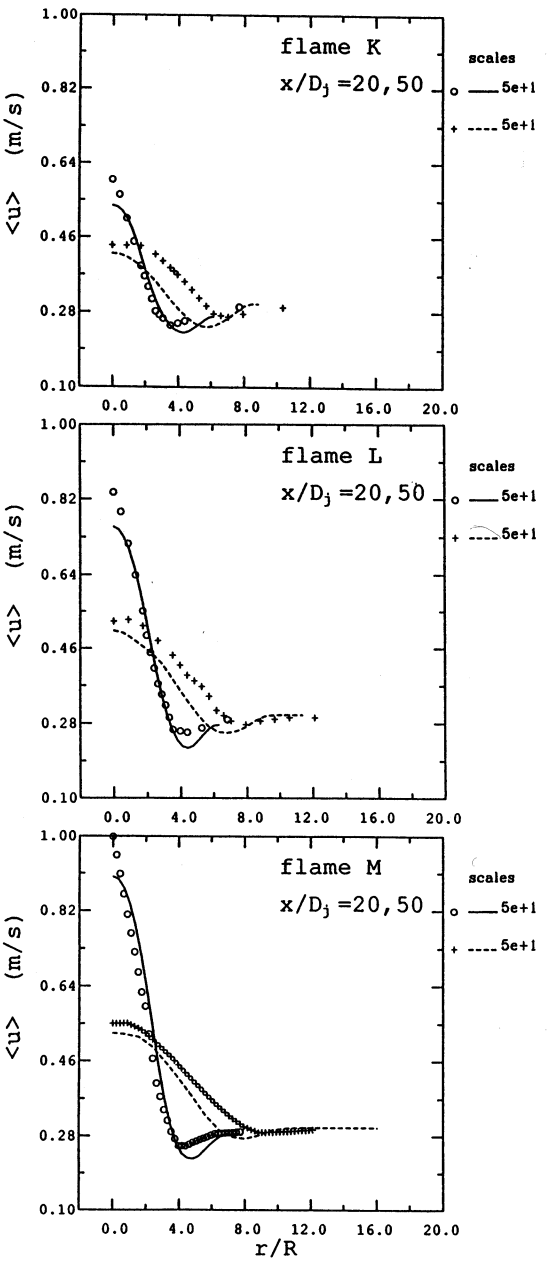

Fig. 4. Measured and calculated radial profiles for the mean axial velocity $\langle u \rangle$ in flames K, L, and M at: ○, —— $x/D_j = 20$; +, ---- $x/D_j = 50$.

profiles for the mean axial velocity, $\langle u \rangle$ and its rms of fluctuations, $\langle u' \rangle$ at various axial locations in the flames. At $x/D_j = 20$, the calculated velocity profiles agree very well with the measurements for all three flames, except very near the centerline

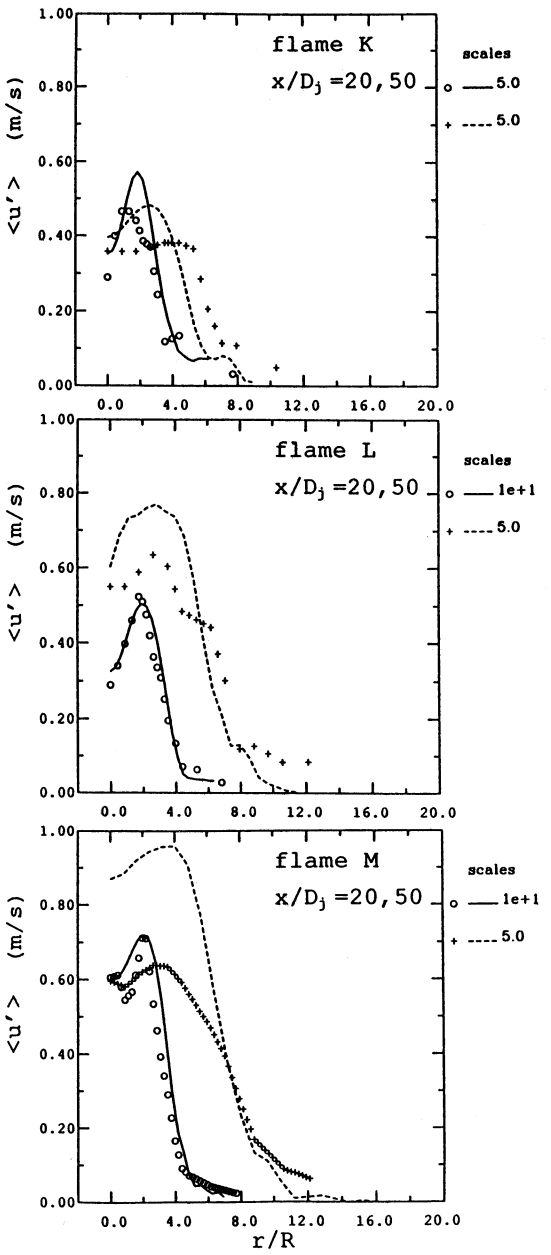

Fig. 5. Measured and calculated radial profiles of the rms of fluctuations of u, $\langle u' \rangle$ in flames K, L, and M at: ○, —— $x/D_j = 20$; +, ---- $x/D_j = 50$.

where the measured values of $\langle u \rangle$ are higher by about 10%. The turbulence profiles almost overlap for flames L and M at $x/D_j = 20$, but not for flame K. Good agreement is also obtained at $x/D_j = 30$. At $x/D_j = 50$, however, the measured profiles of $\langle u \rangle$ are higher than the calculated ones, while the profiles of $\langle u' \rangle$ show the reverse trend. Using the same particle interaction model to perform mixing, Haworth and Pope [27] predicted low values of $\langle u' \rangle$ for a self-similar axisymmetric jet. The discrepancy between the measured and calculated profiles of $\langle u \rangle$ decreases, while that of $\langle u' \rangle$ increases with increasing jet velocity (from flames K to L to M). The velocity deficit, which is mainly due to the momentum deficit caused by the boundary layer on the coflow side, is slightly overpredicted and persists as such up to $x/D_j = 50$ for all flames.

Figure 6 shows the measured and calculated radial profiles for the mean mixture fraction, $\langle \xi \rangle$ at $x/D_j = 20$ and 50 in flames K, L, and M. The agreement is good at $x/D_j = 20$ and 30 (not shown) for all flames, but deteriorates badly at $x/D_j = 50$ where $\langle \xi \rangle$ is overpredicted, and the discrepancy increases from flames K to L to M. Experimental and calculated profiles for the rms of fluctuations of mixture fraction, $\langle \xi' \rangle$ are presented in Fig. 7 for flame L at $x/D_j = 20$ and 30 for flame M at $x/D_j = 20$ and 50. Measurements for $\langle \xi' \rangle$ are not available for flame K and for $x/D_j = 30$ in flame L. The agreement at $x/D_j = 20$ is excellent and is acceptable at $x/D_j = 30$ in flame L. Similarly to $\langle u \rangle$, $\langle u' \rangle$, and $\langle \xi \rangle$, the level of agreements with experiments deteriorates at $x/D_j = 50$.

Radial profiles for the mean density, $\langle \rho \rangle$ are shown in Fig. 8 for $x/D_j = 20$ and 50 in flames K, L, and M. At $x/D_j = 50$, an acceptable level of agreement is obtained between predictions and experiments for all three flames K, L, and M. At $x/D_j = 20$, however, the agreement is good for flame K, but deteriorates progressively for flames L and M. This is expected since, when the jet velocity is increased, the mixing rates become very intense at $x/D_j = 20$ and the chemical kinetic effects become very significant. Such kinetic effects are not addressed in the current model. At $x/D_j = 50$, the mixing rates are relaxed and burning conditions for all flames are not substantially controlled by chemical kinetics.

For all flames investigated in this paper, the good level of agreement obtained at $x/D_j = 20$ and 30 is lost further downstream at $x/D_j = 50$

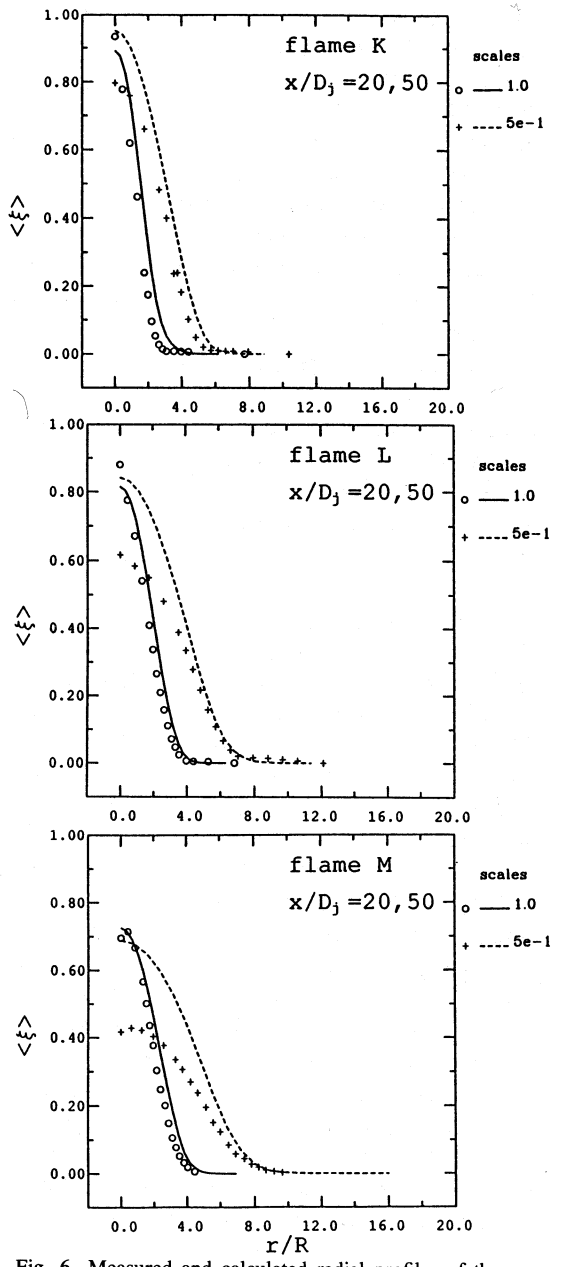

Fig. 6. Measured and calculated radial profiles of the mean mixture fraction, $\langle \xi \rangle$ in flames K, L, and M at: ○, ___ $x/D_j = 20$; +, ---- $x/D_j = 50$.

where the mean mixture fraction, $\langle \xi \rangle$ is overpredicted and the mean velocity, $\langle u \rangle$ is underpredicted. The fluctuating terms, $\langle u' \rangle$ and $\langle \xi' \rangle$ are both overpredicted at $x/D_j = 50$. In an attempt to improve the level of agreement downstream in the flames, the values of the mixing and correlated mixing constants, C_ϕ and $C_{u\phi}$, respectively, have been modified. It is found that while some values of C_ϕ and $C_{u\phi}$ lead to better predictions of the mean terms like $\langle u \rangle$ and $\langle \xi \rangle$, the fluctuating components, $\langle u' \rangle$ and $\langle \xi' \rangle$ become worse. The original values of the constants listed earlier in this paper are maintained.

The main conclusion from these comparisons is that the current pdf method provides an accurate description of the velocity, turbulence, and mixing fields up to $x/D_j \sim 30$. Since these flame locations ($x/D_j = 20$ and 30) are the regions of most interest in the study of turbulence–chemistry interactions, the method provides an adequate framework on which to build a more elaborate thermochemical scheme.

The level of agreement at $x/D_j = 50$ is somewhat disappointing. There are several possible improvements to the modeling that can be expected to reduce the disagreement. Specifically:

(i) the generalized Langevin model [27] is an improvement of the particle-interaction models used for velocity;
(ii) rather than specifying ω as a function of the local mean velocity profile, it can be obtained from an integral equation, or from a partial differential equation [30];
(iii) a more realistic model of molecular mixing [31] could be used.

Statistics of Temperature and Mass Fractions

Calculations for counterflow laminar diffusion flames of methane show that the change in temperature and flame composition with different stretch rates is moderate. Increasing the nominal stretch rate, a from 1 s^{-1} to 350 s^{-1} (flame extinction occurs at 360 s^{-1}) leads to a decrease in the peak temperature [22] from 2197 K to 1840 K. The properties of a single laminar flame with a stretch rate of $a = 100$ s^{-1} are tabulated and used in the current calculations. At $a = 100$ s^{-1}, the peak temperature is 2067 K, which is within $\pm 10\%$ of the peak temperature extremes at $a = 1$ s^{-1} and 350 s^{-1}. Density, temperature, and the mass fractions of CH_4, O_2, CO, CO_2, H_2, H_2O, and N_2

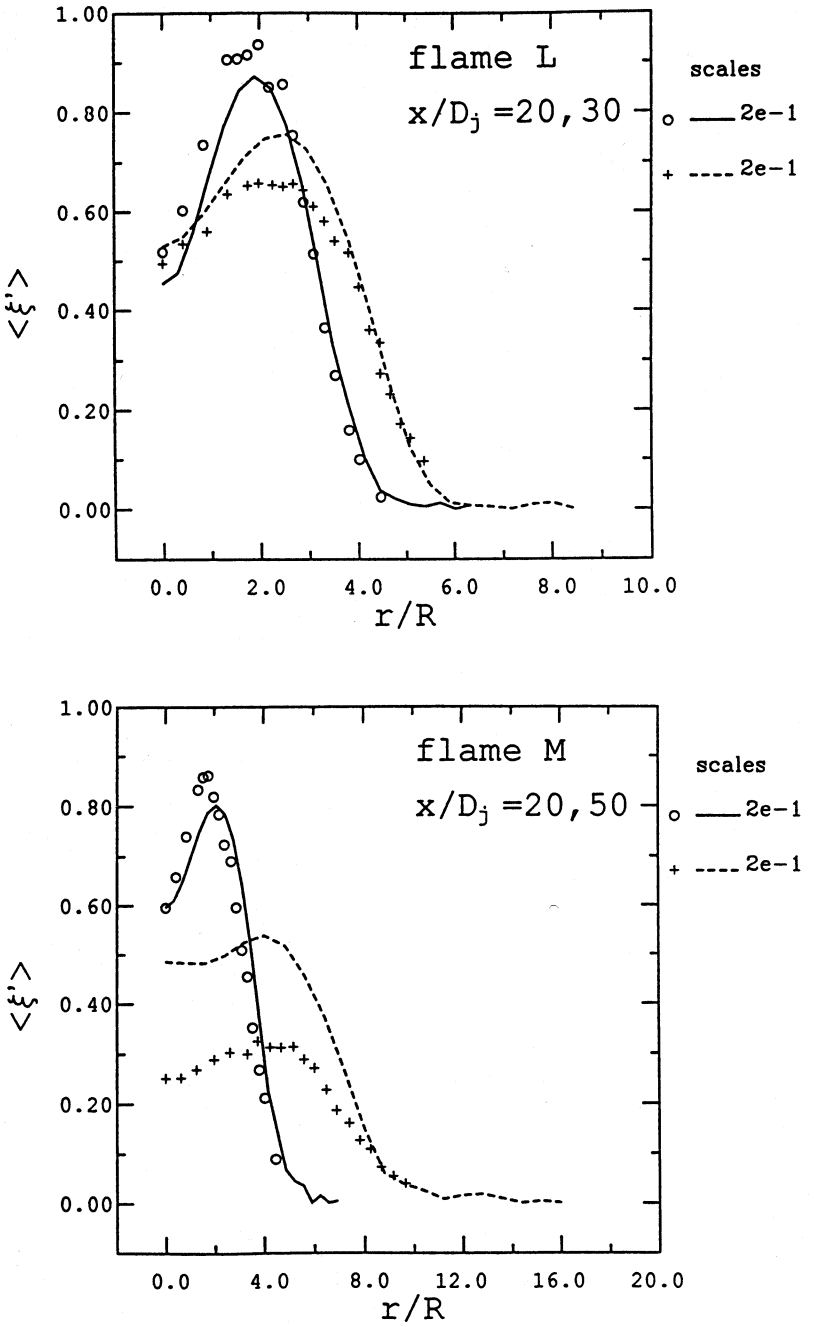

Fig. 7. Measured and calculated radial profiles of the rms of fluctuations of mixture fraction, $\langle \xi' \rangle$ in flame L at: ○, —— $x/D_j = 20$; +, ---- $x/D_j = 30$ and in flame M at: ○, —— $x/D_j = 20$; +, ---- $x/D_j = 50$.

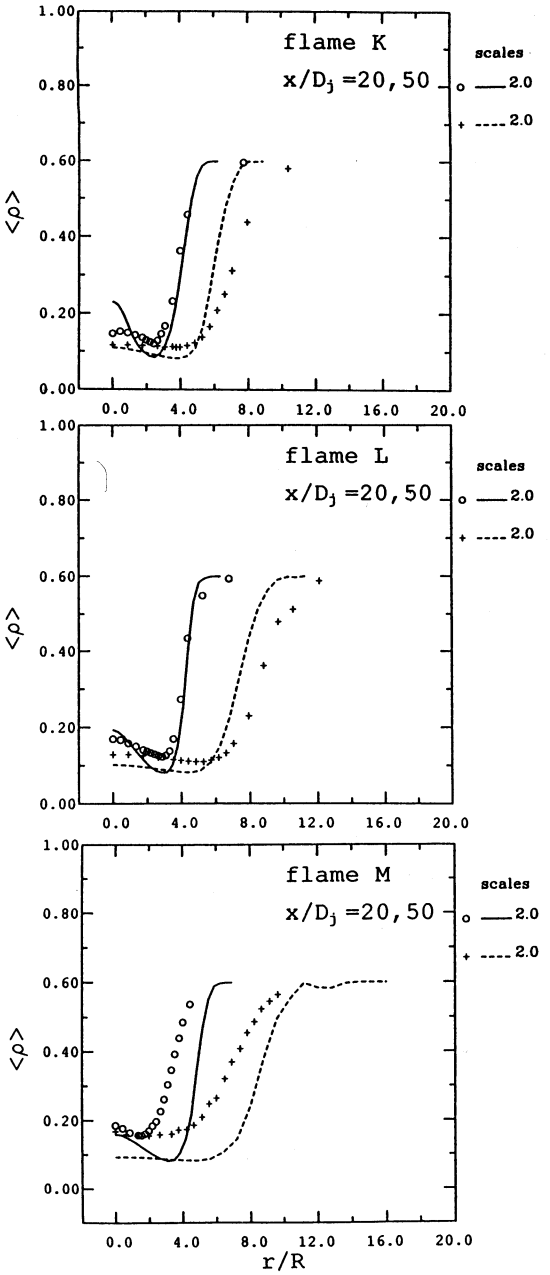

Fig. 8. Measured and calculated radial profiles of the mean density, $\langle\rho\rangle$ (kg/m^3) in flames K, L, and M at: ○, —— $x/D_j = 20$; +, ---- $x/D_j = 50$.

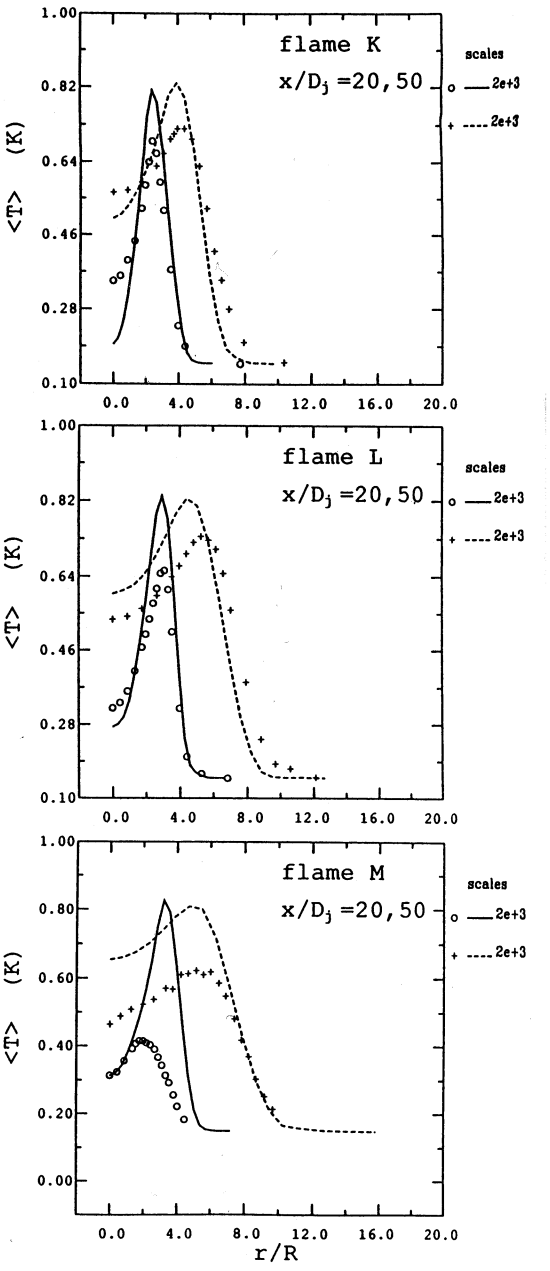

Fig. 9. Measured and calculated radial profiles of the mean temperature, $\langle T\rangle$ in flames K, L, and M at: ○, —— $x/D_j = 20$; +, ---- $x/D_j = 50$.

are tabulated at various values of mixture fraction ranging from 0 to 1. In stretched laminar flamelet modeling, a library of flamelets at various stretch rates are tabulated and a scalar dissipation rate, χ is assigned to each particle according to an assumed distribution for the pdf of χ. The particle is assumed to be extinguished if its value of χ exceeds a critical value χ_q. Haworth *et al.* [15, 16] used this method to model turbulent flames of $CO/H_2/N_2$ fuels and found that at least for the pre-

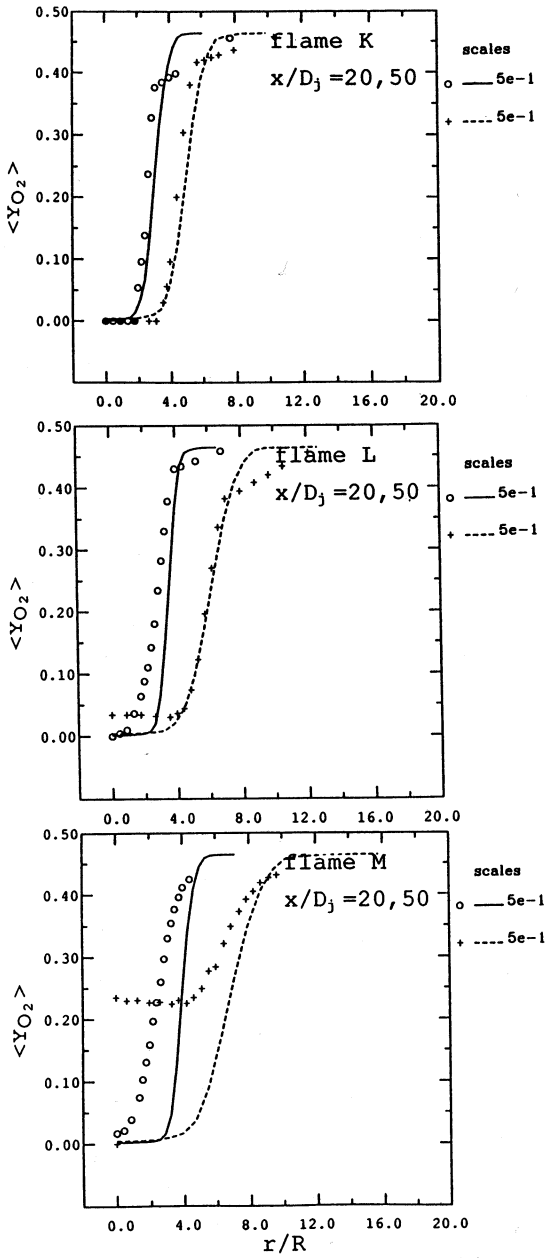

Fig. 10. Measured and calculated radial profiles of the mean mass fraction of O_2, $\langle Y_{O_2} \rangle$ in flames K, L, and M at: ○, — — $x/D_j = 20$; +, ---- $x/D_j = 50$.

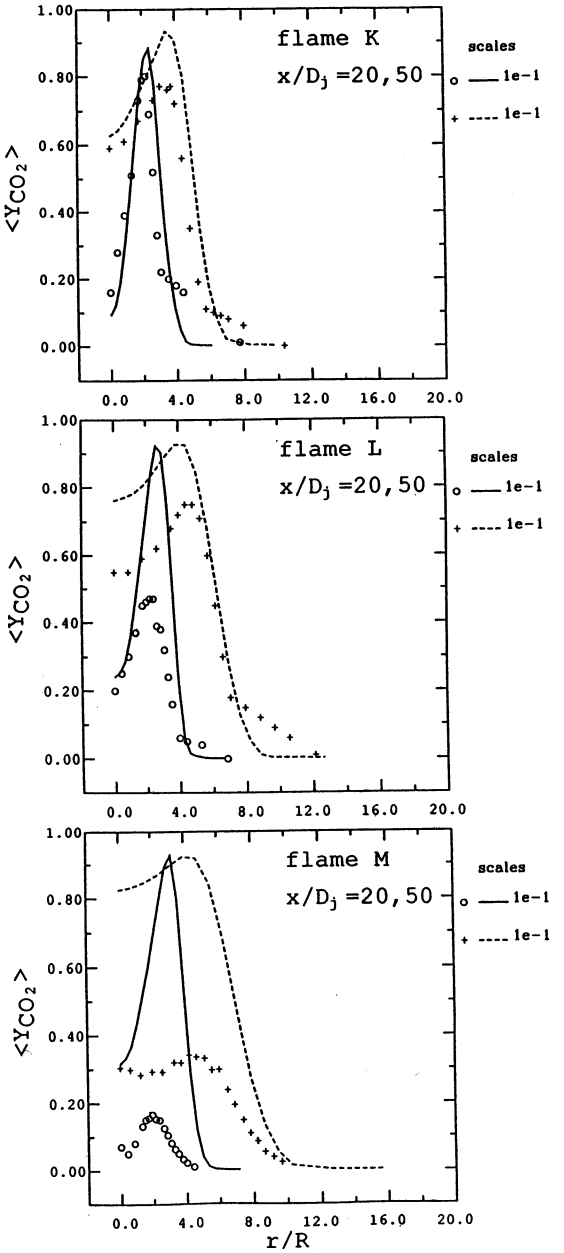

Fig. 11. Measured and calculated radial profiles of the mean mass fraction of CO_2, $\langle Y_{CO_2} \rangle$ in flames K, L, and M at: ○, —— $x/D_j = 20$; +, ---- $-x/D_j = 50$.

diction of OH concentrations, the use of a single flamelet with moderate stretch rate will reproduce the experimental data as well as the multistretched flamelets approach.

The use of the flamelet model in this paper does not imply that such a model accurately describes the physics of combustion in turbulent nonpremixed flames. It is simply intended to demonstrate that this method, like method I, gives relatively good predictions for slowly stretched

flames, but fails when the flames are near blow off and chemical kinetic effects are substantial. Comparisons between the measured and calculated mean temperature and mass fractions of O_2 and CO_2 are presented in this paper. Probe measurements are shown for flames K and L and Raman measurements for flame M.

Figure 9 shows radial profiles of mean temperature $\langle T \rangle$ for flames K, L, and M at $x/D_j = 20$ and 50. For flame K, the calculated peak temperature is higher than the measured one by about 200 K. This in part is due to radiation losses which have not been compensated for in the thermocouple measurements. This discrepancy increases substantially in flame M to about 1000 K at $x/D_j = 20$ and 400 K at $x/D_j = 50$. A similar trend is observed for the mean mass fractions of O_2 and CO_2, $\langle Y_{O_2} \rangle$ and $\langle Y_{CO_2} \rangle$ presented in Figs. 10 and 11, respectively. The remarkably good predictions for flame K deteriorate progressively for flames L and M where $\langle Y_{O_2} \rangle$ is underpredicted and $\langle Y_{CO_2} \rangle$ is overpredicted.

It is evident that a realistic treatment of the chemistry as well as the physics in modeling turbulent combustion is essential, but difficult. Two approaches are possible with pdf methods. The first is the stretched laminar flamelet approach which has been used by Haworth *et al.* [15] with some success in predicting nonpremixed flames of $CO/H_2/N_2$ fuels. The laminar flamelet approach assumes implicitly that for a local fluid mixture, when the scalar dissipation rate, χ changes, the instantaneous thermochemical state changes instantaneously to the new steady-state laminar flame structure. Haworth *et al.* [16] have recognized that this, in fact, is not the case and have analyzed the transient response of flamelets to arbitrary time-dependent strain rates. They have then modified the flamelet model to account for time-dependent flamelet structures and obtained substantial improvements on the previous calculations of Ref. 15.

An alternative approach is to treat the chemical kinetics directly. This is a major advantage of pdf methods since chemical reactions appear in closed form in the pdf transport equation regardless of the complexity of the reaction scheme. The limitations, however, are in the computer time and memory required to solve for a large number of composition variables. A detailed kinetic scheme for methane consists of about 122 reactions and 24 species. This is a tall order for current computers. The three- or four-step mechanisms which are reduced systematically from the detailed schemes [5, 6] are promising since they are computationally feasible and still predict the correct flame structure. The four-step mechanisms predict flame extinction with good accuracy. Such schemes could be efficiently incorporated with the pdf method by tabulating the source term $S_\alpha(\Psi)$ for the relevant composition variables. This is described in detail in a forthcoming paper [32].

CONCLUSIONS

(i) A transport equation for the velocity-composition joint pdf is solved by the Monte Carlo method to calculate the structure of pilot-stabilized turbulent nonpremixed flames.

(ii) The initial conditions (at the jet exit plane) and boundary conditions (in the coflowing stream) are specified following measured profiles. A new model is used for the turbulent frequency to suit the new flow geometry.

(iii) The mean velocity, turbulence, and mixing fields are predicted reasonably well for axial locations up to $x/D_j \sim 30$. The agreement with the measured profiles is less satisfactory at $x/D_j = 50$.

(iv) Recently developed pdf models with a superior treatment for velocity and scalar mixing and for turbulent frequency should improve these calculations.

(v) For flames with methane fuel, simple models for thermochemistry (with density obtained either from laminar flamelet solutions or from a piecewise linear function) give good predictions for the slowly mixing flames (flame K). The predictions are not good for intensely mixed flames where localized extinction occurs.

(vi) In future work [32], realistic chemistry with three- or four-step chemical kinetic schemes will be implemented in the joint pdf calculations to predict finite rate kinetic effects.

Prof. Pope is supported in part by the National Science Foundation (Grant CBT-8814655) and in part by the U.S. Air Force Wright Aeronautical Laboratory, Wright-Patterson AFB, under Contract No. F33615-87-C-2821. Dr. Masri is supported by the Henry Bertie and Florence Mabel Gritton Post-doctoral Fellowship granted by the University of Sydney.

REFERENCES

1. Bilger, R. W., *Turbulent Reacting Flows* (P. A. Libby and F. A. Williams, Eds.), *Topics in Applied Physics*. Springer, 1980, Vol. 44, p. 65.
2. Faeth, G. M., and Samuelsen, G. S., *Prog. Energy Combust. Sci.* 12:305 (1986).
3. Janicka, J., and Kollmann, W., in *Seventeenth Symposium (International) on Combustion*. The Combustion Institute, Pittsburgh, PA, 1979, p. 421.
4. Bilger, R. W. and Stårner, S. H., *Combust. Flame* 51:155 (1983).
5. Bilger, R. W., Stårner, S. H. and Kee, R. J., "On Reduced Mechanisms for Methane–Air Combustion in Nonpremixed Flames", *Combust. Flame*, in press.
6. Peters, N., *Numerical Simulation of Combustion Phenomena* (R. Glowinski, B. Larrouturou, and R. Temam, Eds.), *Lecture Notes in Physics*. Springer, 1985, Vol. 241, p. 90.
7. Janicka, J., Kolbe, W. and Kollmann, W., *J. Nonequil. Thermodyn.* 4:47 (1979).
8. Pope, S. B., *Combust. Sci. Technol.* 25:159 (1981).
9. Pope, S. B., in *Eighteenth Symposium (International) on Combustion*. The Combustion Institute, Pittsburgh, PA, 1981, p. 1001.
10. Nguyen, T. V. and Pope, S. B., *Combust. Sci. Technol.* 42:13 (1984).
11. Chen, J-Y., Kollmann, W. and Dibble, R. W., *Combust. Sci. Technol.* 64:315 (1989).
12. Chen, J-Y. and Kollmann, W., in *Twenty-Second Symposium (International) on Combustion*, The Combustion Institute, Pittsburgh, PA, p. 645.
13. Pope, S. B., *Prog. Energy Combust. Sci.* 11:119 (1985).
14. Pope, S. B. and Correa, S. M., in *Twenty-First Symposium (International) on Combustion*, The Combustion Institute, Pittsburgh, PA, p. 1341.
15. Haworth, D. C., Drake, M. C., and Blint, R. J., *Combust. Sci. Technol.* 60:287 (1988).
16. Haworth, D. C., Drake, M. C., Pope, S. B., and Blint, R. J., in *Twenty-Second Symposium (International) on Combustion*, The Combustion Institute, Pittsburgh, PA, p. 589.
17. Masri, A. R., Dibble, R. W., and Bilger, R. W., *Combust. Flame* 71:245 (1988).
18. Masri, A. R., Bilger, R. W., and Dibble, R. W., *Combust. Flame* 73:261 (1988).
19. Masri, A. R., Bilger, R. W., and Dibble, R. W., *Combust. Flame* 74:267 (1988).
20. Bray, K. N. C., *Numerical Simulation of Combustion Phenomena* (R. Glowinski, B. Larrouturou, and R. Temam, Eds., *Lecture Notes in Physics*, Springer, 1985, Vol. 241, p. 3.
21. Peters, N., in *Twenty-First Symposium (International) on Combustion*, The Combustion Institute, Pittsburgh, PA, 1988, p. 1231.
22. Miller, J. A., Kee, R. J., Smooke, M. D., and Grcar, J. F., Western States Section, The Combustion Institute, Paper WSS/CI 84-10, 1984.
23. Masri, A. R. and Bilger, R. W., in *Twenty-First Symposium (International) on Combustion*, The Combustion Institute, Pittsburgh, PA, 1988, p. 1511.
24. Pope, S. B., *AIAA J.* 22:896 (1984).
25. Pope, S. B., *Combust. Sci. Technol.* 28:131 (1982).
26. Pope, S. B., *Phys. Fluids* 26:3448 (1983).
27. Haworth, D. C. and Pope, S. B., *Phys. Fluids* 30:1026 (1987).
28. Haworth, D. C. and Pope, S. B., *Journal of Computational Physics* 72:311 (1987).
29. Pope, S. B. and Gadh, R., *Commun. Statist.-Simula.* 17(2):349 (1988).
30. Anand, M. S., Pope, S. B., and Mongia, H. C., in *Seventh Symposium on Turbulent Shear Flows*, to appear.
31. Pope, S. B. and Norris, A. T., "Turbulent Mixing Model Based on Ordered Pairing", *Combust. Flame*, to appear.
32. Pope, S. B. and Masri, A. R., in preparation.

Received 26 January 1989; revised 6 June 1989